# Water-Soluble, Unimolecular Containers Based on Amphiphilic Multiarm Star Block Copolymers

**Georg Kreutzer,[†] Céline Ternat,[‡] Tuan Q. Nguyen,[†] Christopher J. G. Plummer,[‡] Jan-Anders E. Månson,[‡] Valeria Castelletto,[§] Ian W. Hamley,[§] Frank Sun,[⊥] Sergei S. Sheiko,[⊥] Andreas Herrmann,[#] Lahoussine Ouali,[#] Horst Sommer,[#] Wolfgang Fieber,[#] Maria Inés Velazco,[#] and Harm-Anton Klok*[,†]**

*Ecole Polytechnique Fédérale de Lausanne (EPFL), Institut des Matériaux, Laboratoire des Polymères, Bâtiment MX-D, CH-1015 Lausanne, Switzerland; Ecole Polytechnique Fédérale de Lausanne (EPFL), Institut des Matériaux, Laboratoire de Technologie des Composites et Polymères, Bâtiment MX-G, CH-1015 Lausanne, Switzerland; Department of Chemistry, University of Reading, Reading, RG6 6AD, United Kingdom; Department of Chemistry, University of North Carolina at Chapel Hill, CB# 3290, Chapel Hill, North Carolina 27599-3290; and Firmenich SA, Division Recherche et Développement, B.P. 239, CH-1211 Genève 8, Switzerland*

*Received March 12, 2006; Revised Manuscript Received April 22, 2006*

ABSTRACT: A new class of water-soluble, amphiphilic star block copolymers with a large number of arms was prepared by sequential atom transfer radical polymerization (ATRP) of *n*-butyl methacrylate (BMA) and poly(ethylene glycol) methyl ether methacrylate (PEGMA). As the macroinitiator for the ATRP, a 2-bromoisobutyric acid functionalized fourth-generation hyperbranched polyester (Boltorn H40) was used, which allowed the preparation of star polymers that contained on average 20 diblock copolymer arms. The synthetic concept was validated by AFM experiments, which allowed direct visualization of single molecules of the multiarm star block copolymers. DSC and SAXS experiments on bulk samples suggested a microphase-separated structure, in agreement with the core−shell architecture of the polymers. SAXS experiments on aqueous solutions indicated that the star block copolymers can be regarded as unimolecular micelles composed of a PBMA core and a diffuse PPEGMA corona. The ability of the polymers to encapsulate and release hydrophobic guests was evaluated using $^1$H NMR spectroscopy. In dilute aqueous solution, these polymers act as unimolecular containers that can be loaded with up to 27 wt % hydrophobic guest molecules.

## Introduction

Many dyes, drugs, fragrances, and flavors are hydrophobic molecules that are sparsely water-soluble. In addition, these molecules are often sensitive toward hydrolytic, enzymatic, and oxidative degradation. Many applications, however, require that these molecules are dispersed in aqueous media. This is often achieved by encapsulating them in the lipophilic core of micelles formed by low molecular weight surfactants or amphiphilic block copolymers.[1,2] A major drawback of such self-assembled nanocontainers is the burstlike release of guest molecules that can occur on dilution below the critical micelle concentration.[3] Furthermore, surfactant and block copolymer micelles can be sensitive to changes in solvent composition, pH, and temperature.

An interesting alternative to surfactant and block copolymer micelles is unimolecular containers obtained via surface functionalization of dendrimers or hyperbranched polymers.[3−13] Because of their covalent nature, these nanocontainers do not dissociate upon dilution and are robust to environmental changes. However, the synthesis of such water-soluble core−shell architectures, especially when they are based on perfect dendrimers, can be rather laborious. Moreover, since the typical size of a dendrimer does not exceed 20 nm, the volume fraction of the lipophilic core and the hydrophilic shell can only be engineered to a limited extent.

Another class of macromolecules that is of potential interest for the development of water-soluble unimolecular containers are amphiphilic star block copolymers. Amphiphilic star block copolymers can be prepared according to two principally different routes. The first is the so-called "grafting from" strategy, which uses a multifunctional core as the initiator for a variety of "living"/controlled polymerization reactions. The second possibility involves coupling of end-reactive polymer molecules onto a multifunctional core ("grafting onto"). Combinations of these two strategies are also possible. In either case, amphiphilic star block copolymers offer the great advantage over surface-modified dendrimers that the absolute and relative sizes of the hydrophobic core and the hydrophilic shell can be conveniently tailored over a much wider range using appropriate controlled/"living" polymerization techniques. So far, a number of amphiphilic water-soluble star block copolymers have been prepared, using various synthetic methods, including anionic polymerization, ring-opening polymerization (ROP), atom transfer radical polymerization (ATRP), or combinations of these techniques.[14−18] A critical parameter in the design of unimolecular containers based on amphiphilic star block copolymers is the number of arms. Depending on the relative volume fractions of the lipophilic and hydrophilic blocks and the number of arms, water-soluble (amphiphilic) star (block co)polymers may lose their individual character and form aggregates instead.[19−24] Although a number of water-soluble amphiphilic star block copolymers have already been prepared, surprisingly

[†] Institut des Matériaux, Laboratoire des Polymères.
[‡] Institut des Matériaux, Laboratoire de Technologie des Composites et Polymères.
[§] University of Reading.
[⊥] University of North Carolina at Chapel Hill.
[#] Firmenich SA, Division Recherche et Développement.
* Corresponding author: e-mail harm-anton.klok@epfl.ch, Fax +41 21 693 5650.

10.1021/ma060548b CCC: $33.50 
Published on Web 05/25/2006

little attention has been paid to their host−guest properties. Leroux et al. reported the synthesis of a series of 4-arm amphiphilic star triblock copolymers prepared from ethyl methacrylate, *tert*-butyl methacrylate, and poly(ethylene glycol) methacrylate and found that the polymers with the highest proportion of hydrophobic monomers formed aggregates in aqueous solution.[25] Very recently, Wang et al. prepared and evaluated a 16-arm amphiphilic star block copolymer based on a lipophilic poly($\epsilon$-caprolactone) (PCL) core and a water-soluble poly(ethylene glycol) (PEG) shell as a drug carrier.[26] These authors found drug loading capacities of up to 22 wt %. The PCL-*b*-PEG multiarm star polymer, however, did not exclusively form unimolecular micelles but was also found to self-assemble into larger aggregates.

In this contribution, we report the synthesis and characterization of a new class of amphiphilic multiarm star block copolymers. The synthesis of the polymers involved consecutive ATRP of *n*-butyl methacrylate (BMA) and poly(ethylene glycol) methyl ether methacrylate (PEGMA), using a 2-bromoisobutyric acid modified hyperbranched polyester (Boltorn H40) as the macroinitiator. The use of such a multifunctional macroinitiator allowed the preparation of star polymers that contain significantly more arms compared to most systems that have been reported to date, which is expected to be beneficial to explore the unimicellar characteristics of these polymers for encapsulation and release applications.

## Experimental Section

**Materials.** Boltorn H40 was received from Perstorp (Perstorp, Sweden) and dried under high vacuum at room temperature for 48 h prior to use. Tetrahydrofuran was distilled from sodium benzophenone under nitrogen. Triethylamine was distilled from $CaH_2$. 2-Bromoisobutyryl bromide (98%, Aldrich), CuBr (>98%, Fluka) and all other solvents and reagents were used as received. *N*-Propyl-2-pyridylmethanimine was synthesized from *n*-propylamine and pyridine-2-carboxaldehyde according to the literature.[27] *n*-Butyl methacrylate (BMA) was freshly distilled prior to use. Poly(ethylene glycol) methyl ether methacrylate (PEGMA, $M_n \sim 475$ g/mol) was passed over a short basic alumina column to remove the inhibitors. Benzyl acetate, geraniol (*trans*-3,7-dimethyl-2,6-octadien-1-ol), decanal, and dorisyl (4-*tert*-butylcyclohexyl acetate) were used as received.

**Analytical Methods.** Attenuated total reflection Fourier transform infrared (ATR-FTIR) spectra were recorded on a Nicolet Magna 560 FTIR spectrometer. Elemental analysis was performed at the Mikroanalytisches Laboratorium Ilse Beetz, Kronach, (Germany). Differential scanning calorimetry (DSC) was performed using a TA Instruments DSC Q100. Analyses were carried out between −120 and 120 °C under an inert atmosphere at a heating/cooling rate of 10 °C/min. Glass transition temperatures were determined from the second heating run and were taken as the midpoint of the change in heat capacity. Gel permeation chromatography (GPC) was performed on a Waters Alliance GPCV 2000 system equipped with refractive index, differential viscometer, and light scattering detection. Separation was carried out at 60 °C with TSK-Gel Alpha 3000 + 4000 columns, using DMF + 1 g/L LiBr as eluent, at a flow rate of 0.6 mL/min. Molecular weights were determined using a universal calibration curve, which was created with narrow polydispersity poly(methyl methacrylate) PMMA standards. Results were calculated with the Empower Pro multidetection GPC software (Ver 5.00). The interdetector volume was adjusted from the peak position of uniform PEG oligomers. The volume of the injected loop was 0.214 mL, and the polymer concentration was calculated to give a viscometric signal less than 0.5% of the baseline level. Nuclear magnetic resonance (NMR) spectra were recorded at room temperature on a Bruker Avance 400 spectrometer. $CDCl_3$ and $D_2O$ were used as solvents, and spectra were calibrated using the residual proton or carbon signal of the solvent. Quantitative $^1$H NMR spectra for encapsulation experiments were recorded under the following conditions: PULPROG: zg; TD: 64K; AQ: 5 s; D1: 20 s; SW: 13 ppm. A minimum of 64 scans were recorded. All integrations were done relative to DMSO, which was added as an internal standard. Atomic force microscopy (AFM) topographic images of individual star block copolymer molecules were collected using a Multimode Atomic Force Microscope (Veeco Metrology Group) equipped with a Nanoscope IIIa control station in tapping mode. Silicon cantilevers (Mikromasch) with a resonance frequency of ∼140 kHz and a spring constant of ∼5 N/m were used. The radius of the probe was less than 10 nm. The samples were prepared by spin-casting dilute chloroform solutions onto freshly cleaved mica. To ensure an accurate representation of the molecules and an experimental error <10%, multiple images were collected from different areas of the same sample. Small-angle X-ray scattering (SAXS) experiments were carried out at the ID02 beamline of the European Synchrotron Radiation Facility (ESRF, Grenoble, France). The samples were mounted in sealed 1 mm thick cells, with an inner spacer ring to hold liquids, contained between mica windows. A wavelength $\lambda$ of 1.0 Å and a sample−detector distance $D$ of 1.2 or 6.5 m were used together a two-dimensional CCD camera. SAXS data were corrected for sample transmission, background scattering, and detector response. The data from the two-dimensional area detector were finally converted into one-dimensional intensity profiles by integration in a circular sector. The resulting corrected intensity curves are denoted $I_c(q)$.

**SAXS Theory.** The small-angle X-ray scattering intensity $I(q)$ of an isotropic solution of polydisperse spherical micelles can be written, within the frame of the local monodisperse approximation, as[28]

$$I(q) = k\int_0^\infty P(q,R)\, S(q,R)\, f(R)\, \mathrm{d}R \qquad \text{(I)}$$

where $k$ is a normalization constant proportional to the number density of particles and $R$ is the micellar core radius. $P(q,R)$ is the monodisperse micellar form factor, $S(q,R)$ is the monodisperse intermicellar structure factor, and $f(R)$ is the radius distribution function. For very dilute particle dispersions, $S(q,R) \sim 1$, so that $I(q)$ is dominated by the particle form factor. An explicit expression for $P(q,R)$ is given below. Although $P(q,R)$ describes the micellar structure, the asymptotic behavior of the SAXS curve depends on the roughness of the external surface of the scattering particle, providing complementary information which has to be considered before constructing a model for the form factor. It is expected that for a sharp particle/solvent interface the Porod law ($I(q) \sim q^{-4}$) should be satisfied at high $q$.[29] For particles with a swollen corona, however, the asymptotic behavior of the SAXS intensity deviates from the Porod law. For example, star polymers exhibit a $\sim q^{-2}$ asymptotic behavior when excluded-volume effects are not significant[30] and a $\sim q^{-5/3}$ power-law behavior when the self-avoiding random walk is considered.[31] Additional information about the shape of the scattering particle as a whole can be obtained from the plot of $I(q)$ in a modified Kratky plot ($I(q)$ vs $q^{5/3}$), which exacerbates the differences in scattering between geometries evolving from linear chains to hard spheres.[30] The model used for the particle form factor has to be coherent with the information extracted from the asymptotic behavior of the SAXS curve and the Kratky plot.

In this paper we use a model introduced by Pedersen and Gerstenberg for the form factor of block copolymer micelles (PG model).[32,33] This model considers a homogeneous spherical micelle core, with a corona made by Gaussian chains attached to a core. In this model the monodisperse micellar form factor is written[33]

$$P(q) = N^2\Delta\rho_c{}^2 P_c(q,R_c) + N\Delta\rho_g{}^2 P_g(q,R_g) + N(N-1)\Delta\rho_g{}^2 S_{gg}(q) + 2N^2\Delta\rho_g\Delta\rho_c S_{cg}(q) \qquad \text{(II)}$$

where the subscripts c and g refer to uniform spherical micelle cores (radius $R_c$) and attached Gaussian chains (radius of gyration $R_g$), respectively, and $N$ is the micelle association number. $\Delta\rho_x$ is the

total excess scattering density of a chain in the core ($x$ = c) or in the corona ($x$ = g). The term $P_c(q,R_c)$ in eq II is the normalized self-correlation term for a uniform sphere, and $P_g(q,R_g)$ is the self-correlation term for Gaussian chains.[33] $S_{cg}(q)$ corresponds to the interference cross term between the sphere and the Gaussian chain starting at the surface of the sphere, and $S_{gg}(q)$ is the interference term between the Gaussian chains attached to the surface of a sphere.[33] Polydispersity of the micelles was modeled using a Gaussian distribution for the core micellar radius. The Gaussian distribution function $f(R_c)$ for the micellar core radius, with mean radius $\bar{R}_s$ and width $\partial$, is defined as

$$f(R_c) = (2\pi\partial^2)^{-1/2} \exp[-(R_c - \bar{R}_c)^2/2\partial^2] \quad \text{(III)}$$

The integration in eq I is over $R_c$, since the polydispersity in association number can be accounted for, because $N$ can be written as a function of the micellar core radius and volume of the chains in the core, $V_c$:

$$N = \frac{4\pi R_c^3}{3V_c} \quad \text{(IV)}$$

Seven parameters have been varied during the fittings, three of which have been fixed to a particular value for all the fittings. The four varied parameters were the mean radius $\bar{R}_c$, the radius of gyration of the chains in the corona $R_g$, the excess scattering length density of the blocks in the corona $\Delta\rho_c$, and the width $\partial$. The three fixed parameters were the volume of each hydrated BMA monomer unit in the core $V_{H,BMA}$, the volume of each hydrated PEGMA monomer unit in the corona $V_{H,PEGMA}$, and the displacement of the corona chains from the core surface $\alpha$. In our fittings we used the excess scattering length density of the blocks in the core $\Delta\rho_c = 1.99 \times 10^{-2}$ e/Å$^3$ calculated from the chemical formula for $H_2O$ and the BMA repeat unit. Four parameters were calculated from those obtained in the paragraph above: the aggregation number $N$, the width of the corona $(1 + \alpha)R_g$, the total micellar radius $R_T = \bar{R}_c + (1 + \alpha)R_g$, and the percentage polydispersity $\chi = 100(\partial/\bar{R}_c)$.

**Procedures. Synthesis of the Macroinitiator (H40-MI).** A solution of vacuum-dried Boltorn H40 (2.80 g, corresponding to 25.0 mmol of hydroxyl groups) in dry THF (80.0 mL) was added to a solution of 4-(dimethylamino)pyridine (4.79 g, 39.3 mmol) and triethylamine (2.53 g, 3.48 mL, 25.0 mmol) in dry THF (20 mL) under an inert atmosphere. Then, 2-bromoisobutyric acid bromide (17.24 g, 9.27 mL, 75.0 mmol) was added dropwise at room temperature. After 48 h, precipitated salts were filtered off and the solvent partially evaporated. The residual solution was precipitated into methanol. The precipitate was dried under vacuum. Yield: 3.55 g (54%). $^1$H NMR (400 MHz, $CDCl_3$): 4.40−4.22 (m, 112 H); 1.89 (s, 192 H); 1.25−1.33 (m, 84 H). $^{13}$C NMR (101 MHz, $CDCl_3$): 171.6 (s); 171.4 (s); 170.8 (s); 66.0 (m); 55.4 (s); 46.7 (s); 30.6 (q); 17.8 (q). GPC (DMF): $M_n$ ~12 300 g/mol, $M_w/M_n$ = 1.72.

**Synthesis of the Lipophilic Core (H40-PBMA$_x$).** A flask equipped with a nitrogen inlet was charged with the macroinitiator H40-MI (1.33 g, ~5.00 mmol of initiating groups), toluene (71.1 g), *n*-butyl methacrylate (71.1 g, 500 mmol), CuBr (700 mg, 5.00 mmol), and *N*-propyl-2-pyridylmethanimine (1.48 g, 10.0 mmol). The mixture was subsequently deoxygenated by three freeze−pump−thaw cycles. Polymerization was carried out in a temperature controlled oil bath at 60 °C. After 140 min, the reaction mixture was cooled in an ice bath. The catalyst complex was removed by suction filtration of the reaction mixture through a layer of silica gel (ca. 3 cm) using a small quantity of toluene to rinse the column. The resulting polymer solution was partially evaporated and finally precipitated into methanol (20 times the volume of the reaction mixture). The precipitate was dried under vacuum.

**Synthesis of the Amphiphilic Star Block Copolymers (H40-PBMA$_x$-*b*-PPEGMA$_y$).** A flask equipped with a nitrogen inlet was charged with CuBr (140 mg, 1.00 mmol) and poly(ethylene glycol) methyl ether methacrylate (PEGMA, 23.8 g, 50.0 mmol). After

**Scheme 1**

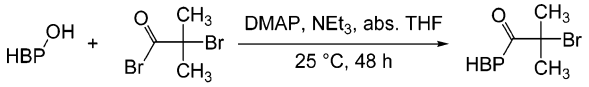


H40-MI

degassing by bubbling nitrogen through the mixture for 30 min, *N*-propyl-2-pyridylmethanimine (369 mg, 380 $\mu$L, 2.50 mmol) was added, and degassing was continued for another 15 min. After that, a previously degassed solution of H40-PBMA$_x$ (2.23 g, ~0.5 mmol of initiating groups) in toluene (23.8 g) was added, and nitrogen purging was continued for 15 min. Finally, the reaction flask was placed in a temperature controlled oil bath at 60 °C. After 5 h, the polymerization was stopped by cooling the reaction mixture to 0 °C. The catalyst was removed by suction filtration through a layer of silica gel (~3 cm) using toluene as a solvent to rinse the column. Subsequently, toluene was evaporated from the resulting polymer solution. The polymer was isolated and purified by repeated precipitation into diethyl ether (20 times the volume of the reaction mixture). Further purification was carried out by dialysis in water (molecular weight cutoff = 10 000 g/mol).

**Alcoholysis of H40-PBMA$_x$.** A solution of sodium 1-butanolate, which had been previously prepared from sodium (690 mg, 30.0 mmol) and THF/1-butanol (v/v = 1/1, 100 mL), was added to a solution of H40-PBMA$_x$ (1.00 g) in dry THF (20.0 mL). The mixture was stirred for 36 h at 25 °C. After that, the THF was evaporated and the residue precipitated into methanol. The precipitate was dried under vacuum. $^1$H NMR spectroscopy and GPC analysis confirmed the formation of linear PBMA$_x$, allowing to calculate the average number of arms per star from GPC molecular weights.

**Encapsulation of Guest Molecules in Aqueous Solution.** Weighed samples of polymer (10/20/30/40 mg) were dissolved in $D_2O$ (1.4 g). Pure $D_2O$ was used as a blank. After the polymer had dissolved, 50 mg of the guest (benzyl acetate, geraniol, dorisyl, or decanal) was added to the solutions. The mixtures were placed on an orbital shaker and agitated for 16 h. After that, samples were filtered into Eppendorf caps through a 0.22 $\mu$m syringe filter and subsequently centrifuged. After centrifugation, aliquots from the water phase were weighed into NMR tubes, and an exact amount of DMSO was added. The following NMR signals were used to determine the total amount of guest molecules in the water phase: benzyl acetate, −(CO)−C*H*$_3$, s, $\delta$ = 2.02−1.81 ppm, depending on type and concentration of polymer; geraniol, C=C*H*−C, t, $\delta$ = 5.3 ppm and/or C=C*H*−C, t, $\delta$ = 5.1 ppm; decanal, −C*H*$_2$−CHO, pert t, $\delta$ = 2.1 ppm in water, 2.31 ppm in polymer solutions; dorisyl, −C(CH$_3$)$_3$, bs, $\delta$ = 0.95−0.80 ppm, depending on polymer concentration. All signals were well separated from the polymer signals except for dorisyl, which limited the accuracy for the experiments. The technique was also used to monitor the release of the volatile guest molecules with time. To this end, a solution with the encapsulated guest was kept at 50 °C. After predetermined periods of time, the evaporated $D_2O$ was replaced in order to maintain the polymer concentration constant, and the total amount of encapsulated guest was determined as mentioned above.

## Results and Discussion

**Synthesis of the Macroinitiator.** The synthesis of the amphiphilic, multiarm star block copolymers started with the modification of the hyperbranched polyester Boltorn H40 with 2-bromoisobutyryl bromide (Scheme 1). This reaction was carried out in dry THF at room temperature in the presence of DMAP and TEA. The complete disappearance of the −C*H*$_2$-OH multiplet, which is found at 3.35−3.60 ppm in the $^1$H NMR spectrum of the H40 precursor, in combination with the appearance of a new signal due to the −C*H*$_3$ groups of the isobutyryl moiety at 1.89 ppm suggested complete conversion of the hydroxyl groups (Figure 1). In addition, the infrared spectrum of the macroinitiator did not show the broad absorption

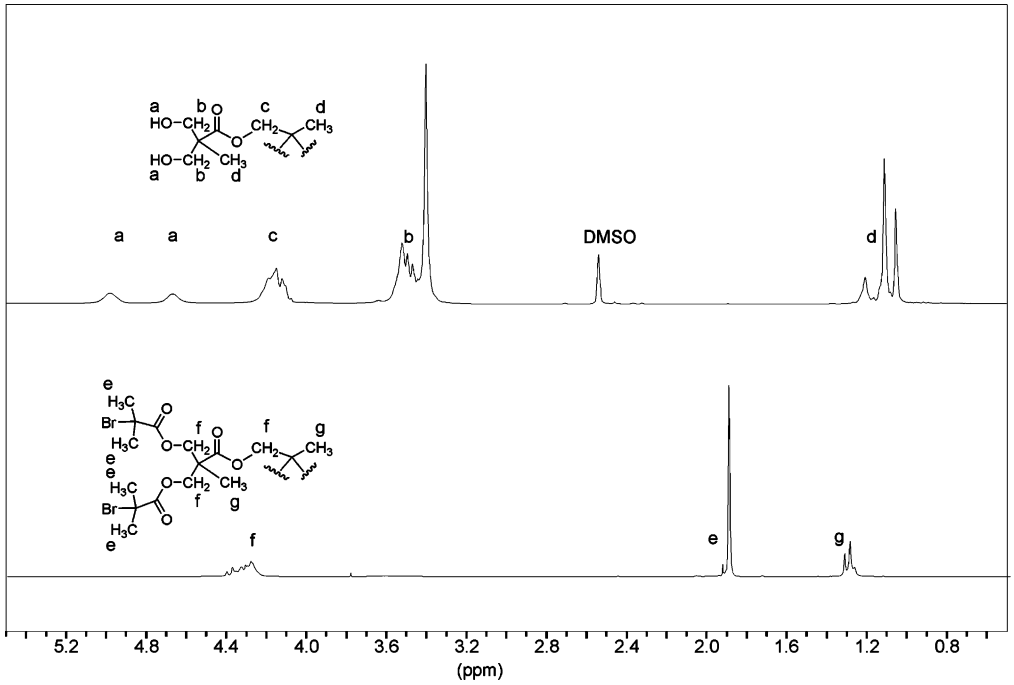


**Figure 1.** $^1$H NMR spectra of H40 (in DMSO-$d_6$, top) and H40-MI (in $CDCl_3$, bottom).

**Chart 1. Representation of an "Average" Fourth-Generation Boltorn H40**

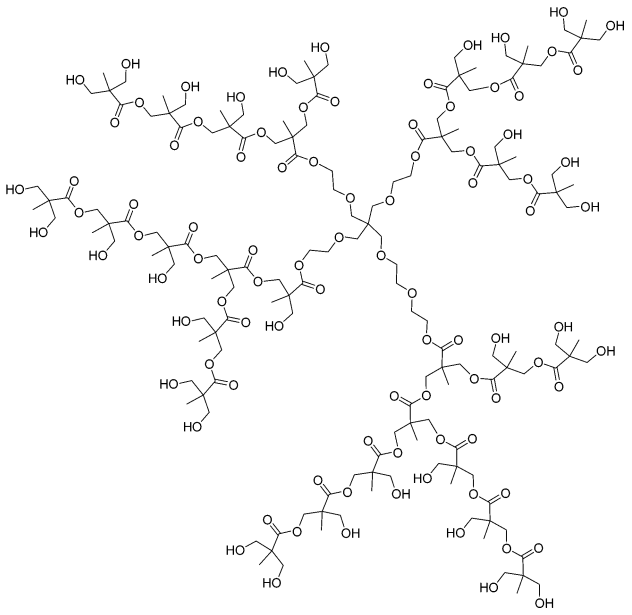

peak at 3100−3500 cm$^{-1}$, which was present in the spectrum of Boltorn H40. Elemental analysis of the H40-MI for bromine gave a bromine content of 30.2 wt %, which is in good agreement with the expected bromine content of 30.5% for complete functionalization of all hydroxyl groups of H40 (Chart 1). The number of hydroxyl groups in H40 can be estimated to 32 by correlating the hydroxyl number of the polymer that is given in the Perstorp data sheet[34] with its GPC molecular weight. Accordingly, the macroinitiator H40-MI contained an average of be 32 2-bromoisobutyryl units that can act as initiators for ATRP. GPC analysis of the H40 and H40-MI revealed an increase in $M_n$ from 3600 to 12 300 g/mol, which is also in good agreement with complete substitution of all hydroxyl functions of H40. The polydispersity of H40-MI was lower than that of H40 (1.72 vs 2.71), presumably due to fractionation that occurred during precipitation.

**Synthesis and Molecular Characterization of the Lipophilic Core.** A potential problem with the synthesis of star polymers using multifunctional initiators is the occurrence of star−star coupling.[35,36] It has been established, however, that this unwanted side reaction can be largely suppressed by restricting the polymerization to relatively low monomer conversion.[35] Well-defined poly(*n*-butyl methacrylate) star polymers (H40-PBMA$_x$) were prepared in toluene using CuBr/*N*-propyl-2-pyridylmethanimine as the catalyst system and H40-MI as initiator (Scheme 2). Using these experimental conditions, a series of three H40-PBMA$_x$ star polymers were synthesized by varying the reaction time. In all cases monomer conversion was kept below 20%. GPC chromatograms of samples taken during the course of the polymerization were monomodal and did not indicate the occurrence of star−star coupling (Figure 2a). Monomer conversion was monitored with $^1$H NMR spectroscopy. Parts b and c of Figure 2 plot $\ln([M]_0/[M])$ vs time and $M_n$ and $M_w/M_n$ vs monomer conversion, respectively. The observed first-order kinetics and linear evolution of molecular weight with conversion are in agreement with the controlled nature of the ATRP process. Figure 2b reveals an induction period of ∼120 min. The occurrence of induction periods that were similar in length have been reported before for ATRP involving structurally related ligands.[37,38] Table 1 provides a summary of the reaction conditions, monomer conversions, and GPC results for each of the three H40-PBMA$_x$ multiarm star polymers. The reported polydispersities (∼1.60) are larger than expected for polymers prepared via ATRP. This is, however, due to the heterogeneity of the macroinitiator, which has a polydispersity of ∼1.7.

To determine the average number of arms per molecule, the H40-PBMA$_x$ star polymers were subjected to alcoholysis with sodium 1-butanolate in a 1-butanol/THF mixture for a period of 36 h at room temperature. According to GPC (Figure 3), this resulted in complete alcoholysis of the H40-PBMA$_x$ star polymers. In this way, for H40-PBMA$_{37}$ the average number of arms per star was estimated to ∼21 using the GPC molecular weights of the PBMA$_x$ arms and H40-PBMA$_x$ stars, which corresponds to an initiator efficiency of ∼57%.

**Scheme 2**

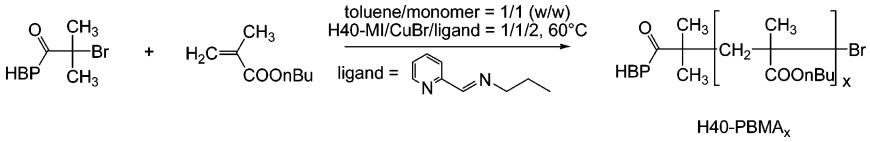


**Synthesis and Molecular Characterization of the Amphiphilic Star Block Copolymers.** Amphiphilic multiarm star block copolymers of PBMA and PPEGMA were prepared via ATRP of PEGMA using H40-PBMA$_x$ as the macroinitiator (Scheme 3). Again, polymerizations were carried out at 60 °C using CuBr/*N*-propyl-2-pyridinylmethanimine as the catalyst system. To avoid star−star coupling, care was taken to keep monomer conversion below 25%. Star block copolymers with various PBMA and PPEGMA block lengths were obtained using different H40-PBMA$_x$ macroinitiators and/or by changing the monomer/initiator ratio. Polymerization conditions for each of these experiments together with GPC data of the resulting polymers are given in Table 2. H40-PPEGMA$_{50}$ is a reference sample that was prepared by polymerization of PEGMA using H40-MI as initiator. GPC chromatograms of samples taken at different intervals during the ATRP of PEGMA using a H40-PBMA$_{15}$ macroinitiator showed a continuous increase in molecular weight and were monomodal, indicating the absence of star−star coupling reactions (Figure 4a). In addition, $^1$H NMR analysis of the monomer consumption as a function of time revealed first-order kinetics, as expected for a controlled radical polymerization process (Figure 4b). The polymerization of PEGMA was preceded by a significant induction period as was also described above for the ATRP of BMA. Initially some of the H40-PBMA$_x$-*b*-PPEGMA$_y$ multiarm star block copolymers were found to cross-link upon storage, both in bulk and in aqueous solution. In bulk, cross-linking occurred within hours, while in solution this process occurred over several days. Cross-linking of PPEGMA containing copolymers has been reported before[39,40] and could be effectively prevented by adding 0.1 wt % 2,6-di-*tert*-butyl-4-methylphenol (BHT) and 4-methoxyphenol (MEHQ) to the samples directly after workup. GPC analysis of multiarm star block copolymers stored in bulk at 2 °C did not reveal any changes in molecular weight and polydispersity, even after 4 months.

Direct proof for the branched architecture of the star block copolymers was obtained from atomic force microscopy (AFM) experiments on monomolecular films. As a representative example, an AFM image of H40-PBMA$_{58}$-*b*-PPEGMA$_{40}$ on mica is shown in Figure 5a. The AFM image clearly shows the individual arms of the star polymers and allows for the

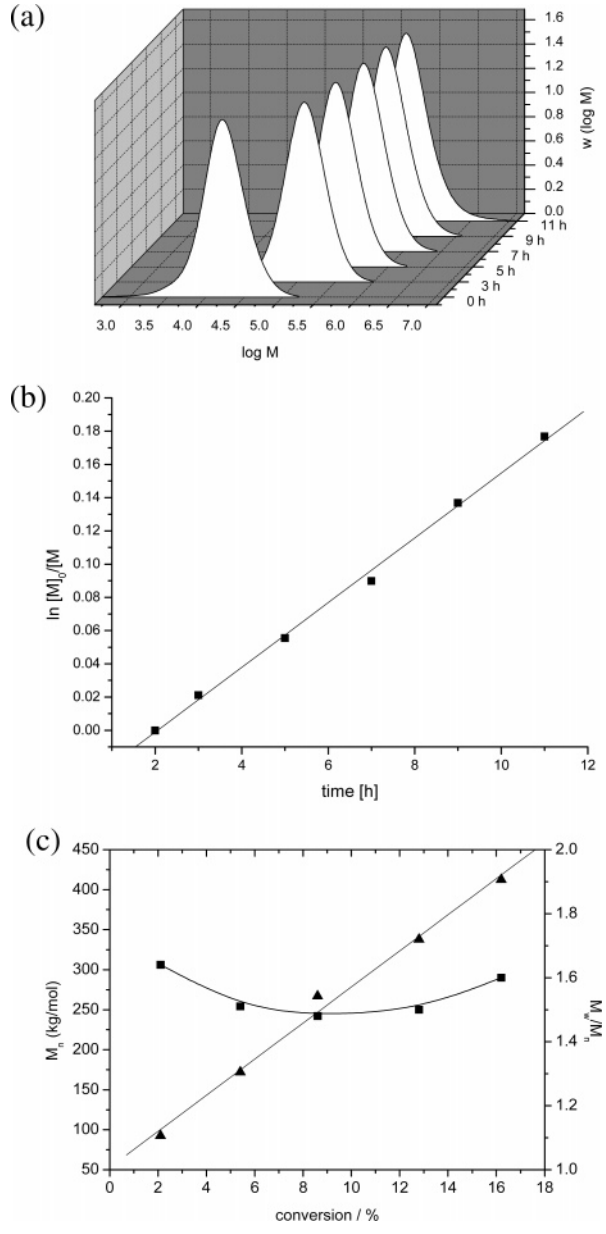


**Figure 2.** (a) GPC traces of samples taken at different time intervals during the ATRP of BMA using H40-MI as the macroinitiator. (b) Kinetic plot for the ATRP of BMA using H40-MI as the macroinitiator. (c) Evolution of number-average molecular weight ($M_n$) and polydispersity ($M_w/M_n$) as a function of conversion for the ATRP of BMA.

**Table 1. Atom Transfer Radical Polymerization of BMA with H40-MI**

| polymer | molar ratio of H40-MI/CuBr/ligand/BMA | BMA conv[a] [%] | $M_n$[b] [g/mol] | $M_w/M_n$[b] | DP$_n$[b] |
|---|---|---|---|---|---|
| H40-PBMA$_{34}$ | 1/1/2/100 | 7.4 | 166 000 | 1.65 | 34 |
| H40-PBMA$_{37}$ | 1/1/2/100 | 11.9 | 182 000 | 1.69 | 37 |
| H40-PBMA$_{58}$ | 1/1/2/100 | 16.8 | 277 000 | 1.88 | 58 |

[a] Determined with $^1$H NMR spectroscopy. [b] Number-average molecular weight ($M_n$), polydispersity ($M_w/M_n$), and number-average degree of polymerization per arm (DP$_n$) assuming a total of 32 arms per molecule.

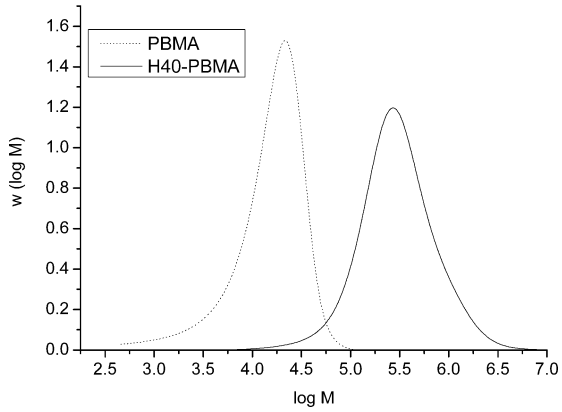


**Figure 3.** GPC molecular weight distributions before and after alcoholysis of the H40 core of H40-PBMA$_{37}$.

**Scheme 3**

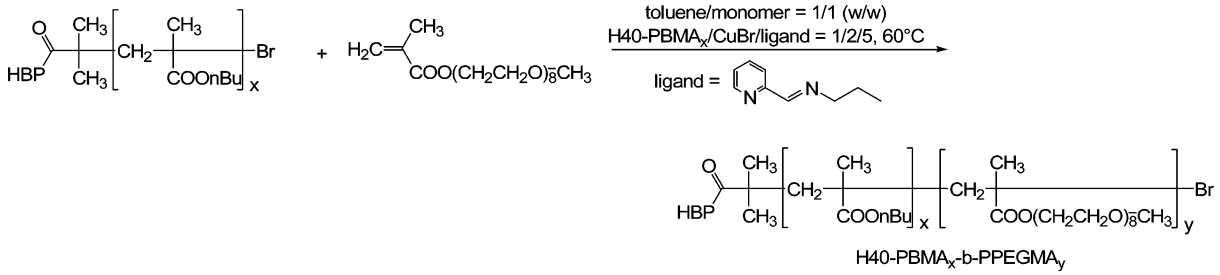


**Table 2. ATRP of PEGMA with H40-PBMA$_x$**

| polymer | molar ratio of H40-PBMA/CuBr/ligand/PEGMA | PEGMA conv [a] [%] | $M_n$ [b] [g/mol] | $M_w/M_n$ [b] | $DP_n$ [b] | $T_g$ [c] [°C] |
|---|---|---|---|---|---|---|
| H40-PBMA$_{37}$-*b*-PPEGMA$_{39}$ | 1/2/4/100 | 18.9 | 782 000 | 2.04 | 39 | −64.1; 12.2 |
| H40-PBMA$_{37}$-*b*-PPEGMA$_{19}$ | 1/2/4/500 | 6.5 | 476 000 | 1.81 | 19 | −63.7; 3.1 |
| H40-PBMA$_{34}$-*b*- PPEGMA$_{23}$ | 1/2/4/250 | 9.2 | 518 000 | 1.66 | 23 | −63.8; 2.6 |
| H40-PBMA$_{58}$-*b*- PPEGMA$_{40}$ | 1/2/4/250 | 26.0 | 879 000 | 1.86 | 40 | −65.2; 13.0 |
| H40−PPEGMA$_{50}$ | 1/2/4/250 | | 780 000 | 1.82 | 50 | −64.9 |

[a] Determined with $^1$H NMR spectroscopy. [b] Number-average molecular weight ($M_n$), polydispersity ($M_w/M_n$), and number-average degree of polymerization per arm ($DP_n$) assuming a total of 32 arms per molecule. [c] From differential scanning calorimetry.

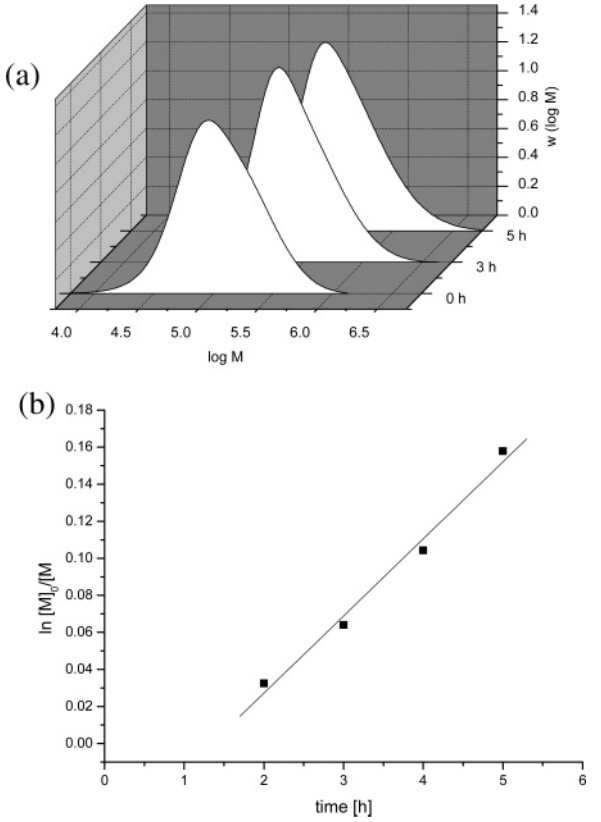


**Figure 4.** (a) GPC traces of samples taken at different time intervals during the ATRP of PEGMA using H40-PBMA$_{15}$ as the macroinitiator. (b) Kinetic plot for the ATRP of PEGMA using H40-PBMA$_{15}$ as the macroinitiator.

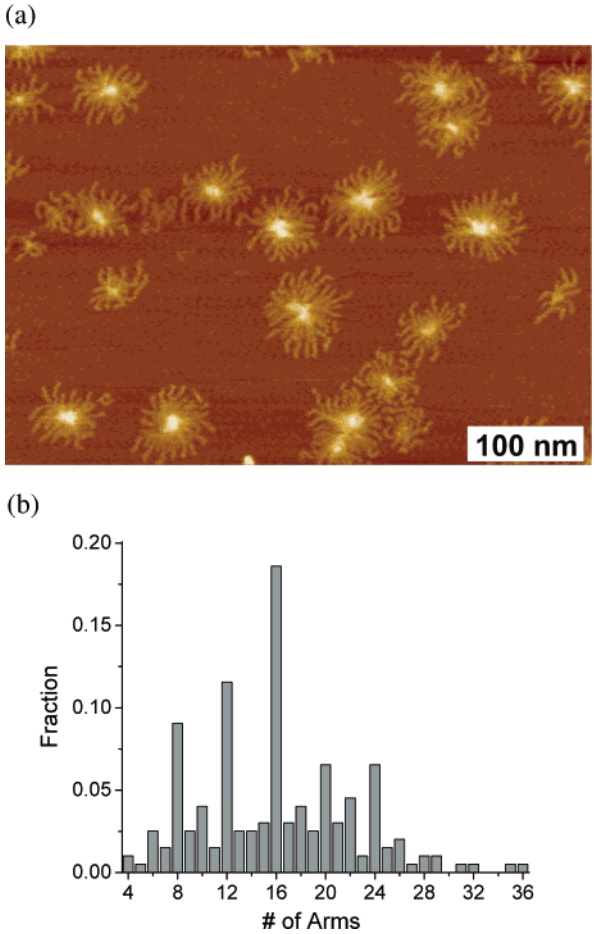


**Figure 5.** (a) Atomic force microscopy height micrograph of H40-PBMA$_{58}$-*b*-PPEGMA$_{40}$. (b) Distribution of the number of arms, as evaluated from AFM images, for H40-PBMA$_{58}$-*b*-PPEGMA$_{40}$.

determination of the exact number of arms per molecule. Figure 5b shows the arm-number distribution obtained after analysis of more than 1000 molecules. The average number of arms is 16, which is only slightly lower than the number determined by alcoholysis of the H40-PBMA$_x$ precursors. Interestingly, the arm number distribution is not continuous but reveals maxima at 8, 12, 16, 20, and 24 arms. These results can be rationalized by considering that the macroinitiator that has been used for the ATRP is a pseudo-fourth-generation, structurally heterogeneous polymer (Chart 1). Because of the 4-fold symmetry of the macroinitiator, star polymers containing a multiple number of 4 arms can be generated from a number of isomeric initiators, which explains the observed relatively high abundance of 8-, 12-, 16-, 20-, and 24-arm star polymers.

**Bulk and Solution Structure and Properties.** The thermal properties of the amphiphilic multiarm star block copolymers were analyzed with DSC. As a representative example, heating

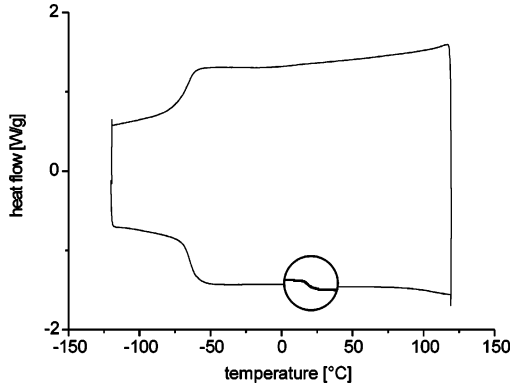


**Figure 6.** DSC traces (second heating and cooling run) of H40-PBMA$_{58}$-*b*-PPEGMA$_{40}$.

and cooling traces of H40-PBMA$_{58}$-*b*-PPEGMA$_{40}$ are shown in Figure 6. For all star block copolymers, two glass transition temperatures ($T_g$'s) were recorded, which are listed in Table 2. A first $T_g$ was observed at ~−65 °C, which is in good agreement with the literature values reported for PPEGMA.[39,40] The second $T_g$ was found between 3 and 13 °C, slightly below the literature value for PBMA.[41] The observation of two distinct $T_g$'s suggests a microphase-separated structure and supports the core−shell structure of the amphiphilic multiarm star block copolymers.

Further evidence for the core−shell topology of the multiarm star block copolymers was obtained from small-angle X-ray scattering (SAXS). As an example, the SAXS pattern obtained from a bulk sample of H40-PBMA$_{37}$-*b*-PPEGMA$_{39}$ is shown in Figure 7a. Although the SAXS pattern only shows a single peak, which is insufficient to unambiguously determine the bulk morphology, it underlines the microphase-separated structure. The domain spacings determined from the SAXS patterns of the different samples are listed in Table 3. To interpret the measured domain spacings in terms of a possible packing model, the end-to-end distances of the PBMA and PPEGMA segments were estimated from molecular modeling using the Hyperchem 7.5 software. For PBMA$_{37}$ and PPEGMA$_{39}$, for example, end-to-end distances of 2.9 nm (PBMA$_{37}$) and 5.6 nm (PPEGMA$_{39}$) were obtained. With these segment lengths, the domain spacings listed in Table 3 can be interpreted as a closely packed organization of star block copolymer molecules with interdigitation of the PPEGMA blocks (Figure 7b). The sum of 2 times the estimated end-to-end distance of the PBMA segment and that of the PPEGMA segment is slightly smaller than the measured *d* spacing (e.g., for H40-PBMA$_{37}$-*b*-PPEGMA$_{39}$ 11.4 nm vs 13.7 nm). This difference is probably due to the more stretched conformation of the PBMA and PPEGMA segments in the star block copolymer as compared to the modeling experiments, which were performed without steric constraints.

In addition to solid samples, also 1 wt % aqueous solutions of the star block copolymers were studied with SAXS. Figure 8 shows the SAXS curves obtained for 1 wt % H40-PBMA$_{37}$-*b*-PPEGMA$_{39}$, H40-PBMA$_{37}$-*b*-PPEGMA$_{19}$, H40-PBMA$_{34}$-*b*-PPEGMA$_{23}$, and H40-PBMA$_{58}$-*b*-PPEGMA$_{40}$ together with a fit of the asymptotic behavior at high *q*. For the different samples, the high *q* dependences of $I(q)$ vary between $q^{-1.4}$ and $q^{-1}$. For a sharp particle/solvent interface, a $q^{-4}$ dependence is expected.[29] For star polymers, instead, the high *q* dependence of $I(q)$ can vary from $q^{-2}$ to $q^{-5/3}$.[30,31] The high *q* dependence of $I(q)$ of the curves in Figure 8 is distinctly different from that expected for a hard particle/solvent interface, suggesting instead a diffuse corona/water interface.

In a first attempt to obtain information about the particle size, the SAXS curves were background corrected, which involved

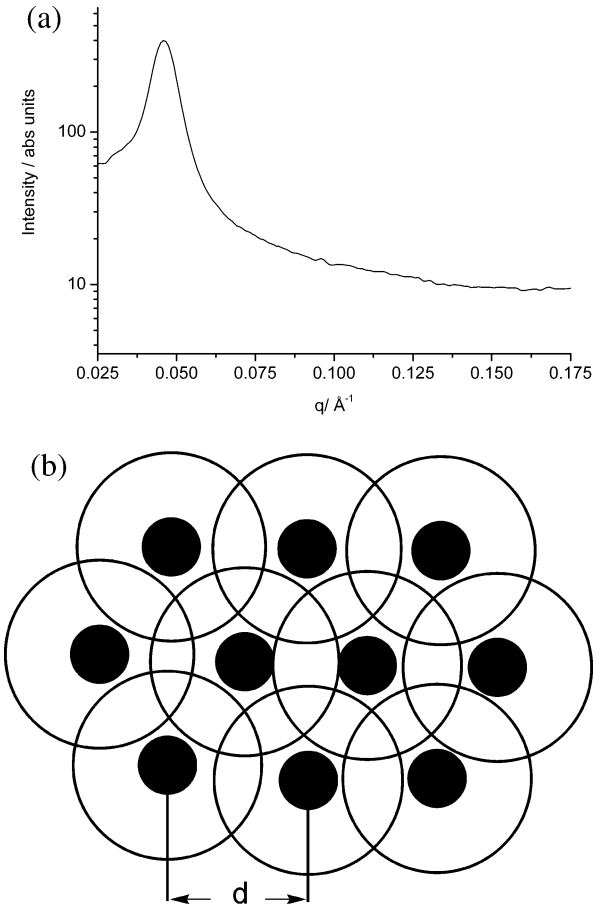


**Figure 7.** (a) Solid-state SAXS intensity profile recorded for H40-PBMA$_{37}$-*b*-PPEGMA$_{39}$. (b) Schematic representation of the bulk microphase-separated structure of the H40-PBMA$_x$-*b*-PPEGMA$_y$ star block copolymers. The black domains represent the PBMA cores and the white domains the PPEGMA corona of the star block copolymers. The hexagonal arrangement of the molecules is idealized and not supported by the SAXS data.

**Table 3. Results of the Bulk SAXS Analysis of the H40-PBMA$_x$-*b*-PPEGMA$_y$ Multiarm Star Block Copolymers**

| polymer | vol % PBMA[a] | vol % PPEGMA[a] | *d*/bulk [nm] |
|---|---|---|---|
| H40-PBMA$_{37}$-*b*-PPEGMA$_{39}$ | 23.8 | 76.2 | 13.7 |
| H40-PBMA$_{37}$-*b*-PPEGMA$_{19}$ | 38.9 | 61.1 | 12.9 |
| H40-PBMA$_{34}$-*b*-PPEGMA$_{23}$ | 32.7 | 67.3 | 12.7 |
| H40-PBMA$_{58}$-*b*-PPEGMA$_{40}$ | 32.1 | 67.9 | 17.7 |
| H40-PPEGMA$_{50}$ | 0.0 | 100.0 | |

[a] Calculated from GPC molecular weights and densities of the polymers ($\rho$(PBMA) = 1.07 g/mL, $\rho$(PPEGMA) = 1.1 g/mL).

subtracting the asymptotic dependence fitted in Figure 8, and were subsequently used to construct the modified Kratky plots shown in Figure 9. Figure 9 shows the experimental data together with the calculated Kratky plots for monodisperse, hard spheres with radii of 122, 110, 107, and 155 Å for H40-PBMA$_{37}$-*b*-PPEGMA$_{39}$, H40-PBMA$_{37}$-*b*-PPEGMA$_{19}$, H40-PBMA$_{34}$-*b*-PPEGMA$_{23}$, and H40-PBMA$_{58}$-*b*-PPEGMA$_{40}$, respectively. Although there is some resemblance between the experimental and calculated Kratky plots, the agreement is not very satisfactory, which reflects the diffuse interface between the PPEGMA corona of the molecules and the surrounding aqueous medium.

Next, the SAXS data were evaluated using the Pedersen−Gerstenberg (PG) model.[32,33] Since this model considers a micelle consisting of a corona with Gaussian chains attached to a central core, it seemed more appropriate to analyze the

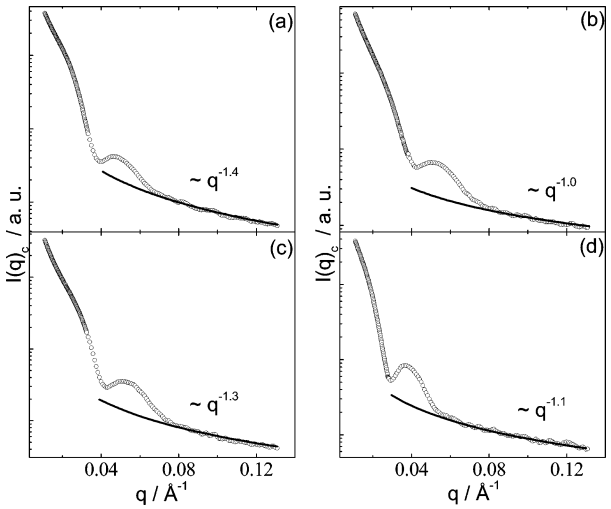


**Figure 8.** SAXS curves for 1 wt % aqueous solutions of (a) H40-PBMA$_{37}$-*b*-PPEGMA$_{39}$, (b) H40-PBMA$_{37}$-*b*-PPEGMA$_{19}$, (c) H40-PBMA$_{34}$-*b*-PPEGMA$_{23}$, and (d) H40-PBMA$_{58}$-*b*-PPEGMA$_{40}$. The full lines correspond to a fitting of the asymptotic behavior of the SAXS curves using $I(q) \sim q^{-\Delta}$. The $\Delta$ coefficient for each SAXS curve is shown in the figure.

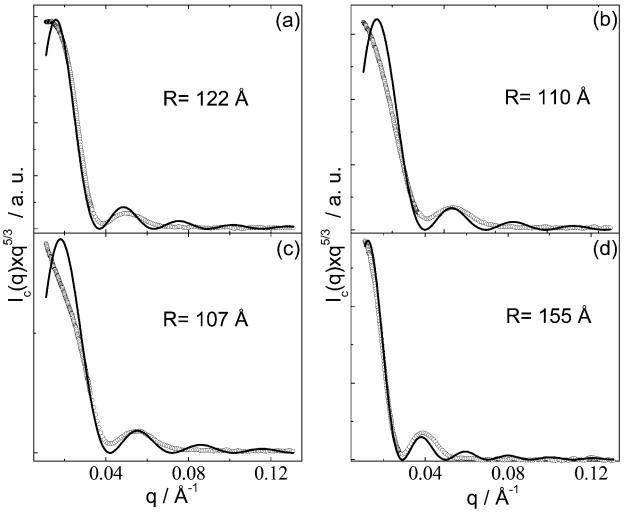


**Figure 9.** Modified Kratky plots for 1 wt % aqueous solutions of (a) H40-PBMA$_{37}$-*b*-PPEGMA$_{39}$, (b) H40-PBMA$_{37}$-*b*-PPEGMA$_{19}$, (c) H40-PBMA$_{34}$-*b*-PPEGMA$_{23}$, and (d) H40-PBMA$_{58}$-*b*-PPEGMA$_{40}$. The asymptotic dependence fitted in Figure 8 has been subtracted from the experimental SAXS curves. The full lines correspond to the modified Kratky plots calculated for hard spheres with radius *R*. The value of *R* used for each SAXS curve is indicated in the figure.

SAXS data than the Kratky model discussed above. Figure 10 shows the experimental SAXS data of the four samples after subtraction of the asymptotic dependence fitted in Figure 8 together with the fitted SAXS curves based on the PG model. The agreement between the experimental and the fitted data is quite good and much better than in Figure 9. This suggests that the H40-PBMA$_x$-*b*-PPEGMA$_y$ star block copolymers may indeed be regarded as unimolecular micelles with a spherical core and a diffuse PPEGMA corona. Over the investigated range of concentrations, the SAXS experiments did not provide any indications for aggregation of the star block copolymers. As mentioned in the Experimental Section, fitting the experimental data with the PG model involves seven parameters, three of which are fixed. These fitting parameters are listed in Table 4. Fitting the experimental SAXS data with the PG model, the parameters from Table 4 were used to calculate the following four parameters: the aggregation number *N*, the width of the

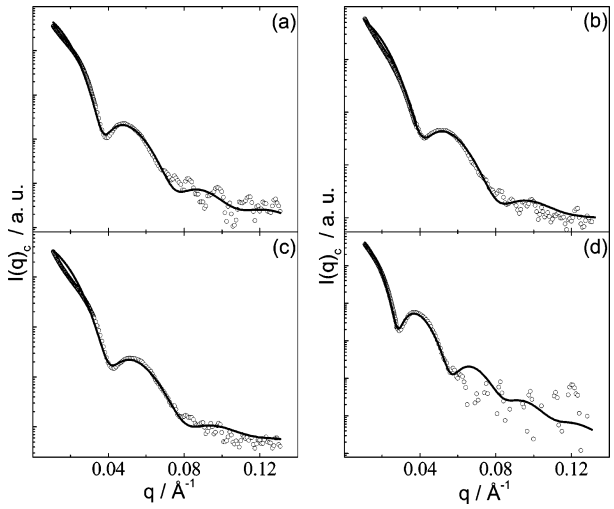


**Figure 10.** SAXS data for 1 wt % aqueous solutions of (a) H40-PBMA$_{37}$-*b*-PPEGMA$_{39}$, (b) H40-PBMA$_{37}$-*b*-PPEGMA$_{19}$, (c) H40-PBMA$_{34}$-*b*-PPEGMA$_{23}$, and (d) H40-PBMA$_{58}$-*b*-PPEGMA$_{40}$. The asymptotic dependence fitted in Figure 8 has been subtracted from the experimental SAXS curves. The full lines correspond to the fitting of the SAXS curves using the PG model. The parameters used for and extracted from the fitting are listed in Tables 4 and 5.

corona $(1 + \alpha)R_g$, the total micellar radius $R_T = \bar{R}_c + (1 + \alpha)R_g$, and the percentage polydispersity, $\chi = 100(\partial/\bar{R}_c)$. These parameters are listed in Table 5.

Tables 4 and 5 show that the core radius $\bar{R}_c$ and the total radius $R_T$ increase with increasing chain length of the PBMA$_x$ segment and the PBMA$_x$-*b*-PPEGMA$_y$ arms, respectively. It is interesting to compare the $R_T$ values in Table 5 with the estimated end-to-end distances of the PBMA$_x$-*b*-PPEGMA$_y$ arms estimated from molecular modeling. For PBMA$_{37}$-*b*-PPEGMA$_{39}$, for example, modeling suggests an end-to-end distance of ~85 Å, while Table 5 indicates $R_T \approx 122$ Å. This difference is probably due to the fact that in the case of the star block copolymers the PBMA$_x$-*b*-PPEGMA$_y$ arms are attached to a central H40 core and in aqueous solutions the PPEGMA blocks are hydrated, which both induce a stretching of the block copolymer arms. Interestingly, the values for $R_T$ in Table 5 are quite close to the radii that were used to model the Kratky plots in Figure 9. The polydispersity of the core ($\chi$) is similar to that found in the literature for other polymer micelles that were analyzed with the PG model.[42] The apparent aggregation numbers (*N*) calculated from the fit of the PG model to the SAXS curves are much higher than the experimentally determined number of arms of the H40-PBMA$_x$-*b*-PPEGMA$_y$ star block copolymers. This discrepancy is most likely due to the fact that the PG model considers self-assembled block copolymer micelles while the investigated H40-PBMA$_x$-*b*-PPEGMA$_y$ star block copolymers consist of amphiphilic diblock copolymer arms, whose PBMA end groups are covalently connected to a multifunctional core.

**Encapsulation and Release Properties.** The ability of the polymers to encapsulate and release hydrophobic guest molecules in aqueous media was investigated by means of $^1$H NMR spectroscopy. Four different guests were investigated: benzyl acetate, geraniol, decanal, and dorisyl (Chart 2). The encapsulation experiments were carried out by saturating a solution of the polymer in $D_2O$ with the guest. After separation of the excess guest, the total amount of guest in the $D_2O$ phase was determined by means of $^1$H NMR spectroscopy. Figure 11a compares the uptake of benzyl acetate by H40-PBMA$_{37}$-*b*-PPEGMA$_{39}$ and H40-PPEGMA$_{50}$. In the case

**Table 4. Parameters Used To Fit the Experimental SAXS Curves in Figure 10 Using the PG Model[a]**

| polymer | $\bar{R}_c$[b] [Å] | $R_g$[b] [Å] | $\Delta\rho_c$[b] [e/Å$^3$] | $\partial$[b] [Å] | $V_{H,BMA}$[c] [Å$^3$] | $V_{H,PEGMA}$[c] [Å$^3$] | $\alpha$[c] |
|---|---|---|---|---|---|---|---|
| H40-PBMA$_{37}$-*b*-PPEGMA$_{39}$ | 49 | 40.3 | $3.59 \times 10^{-1}$ | 5 | 267 | 5207 | 0.8 |
| H40-PBMA$_{37}$-*b*-PPEGMA$_{19}$ | 49 | 30.2 | $2.1 \times 10^{-1}$ | 6 | 267 | 5207 | 0.8 |
| H40-PBMA$_{34}$-*b*-PPEGMA$_{23}$ | 47 | 33.3 | $1.99 \times 10^{-1}$ | 6 | 267 | 5207 | 0.8 |
| H40-PBMA$_{58}$-*b*-PPEGMA$_{40}$ | 75 | 40.3 | $2.6 \times 10^{-1}$ | 8 | 267 | 5207 | 0.8 |

[a] The definition of each of the parameters is given in the Experimental Section. [b] Parameters varied during the fitting to the SAXS curves. [c] Parameters fixed during the fitting to the SAXS curves.

**Table 5. Parameters Calculated from Fitting the Experimental SAXS Data in Figure 10 with the PG Model Using the Parameters from Table 4[a]**

| polymer | $N$ | $(1+\alpha)R_g$ [Å] | $R_T$ [Å] | $\chi$ [%] |
|---|---|---|---|---|
| H40-PBMA$_{37}$-*b*-PPEGMA$_{39}$ | 50 | 73 | 122 | 10 |
| H40-PBMA$_{37}$-*b*-PPEGMA$_{19}$ | 50 | 55 | 104 | 12 |
| H40-PBMA$_{34}$-*b*-PPEGMA$_{23}$ | 45 | 60 | 107 | 13 |
| H40-PBMA$_{58}$-*b*-PPEGMA$_{40}$ | 113 | 73 | 148 | 11 |

[a] The definition of each of the parameters is given in the Experimental Section.

**Chart 2. Guest Molecules Used for the Encapsulation Experiments**

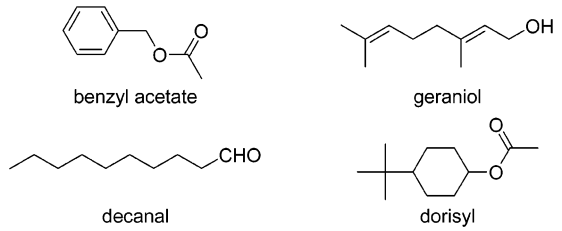


of H40-PPEGMA$_{50}$ increasing the polymer concentration did not result in a significant increase in the amount of fragrance in the aqueous solution. Over the range of polymer concentrations that were investigated, the fragrance concentration was constant around 2 mg/mL, which is close to the intrinsic water solubility of the benzyl acetate (1.5 mg/mL).[43] For the amphiphilic multiarm star block copolymer H40-PBMA$_{37}$-*b*-PPEGMA$_{39}$, however, the amount of benzyl acetate in the aqueous phase increased linearly with increasing polymer concentration. The amphiphilic multiarm star block copolymers could encapsulate significant amounts of fragrance molecules. Loadings of up to 27 wt % benzyl acetate were achieved using H40-PBMA$_{37}$-PPEGMA$_{39}$. Figure 11b shows the uptake of different guests in aqueous solutions of H40-PBMA$_{37}$-*b*-PPEGMA$_{39}$, evidencing the feasibility of the nanocapsules to encapsulate a diverse variety of guest molecules, with different polarity, functionalities, and sterical demand.

Figure 12 compares the benzyl acetate release at 50 °C from 20 mg/mL aqueous solutions of H40-PPEGMA$_{50}$ and H40-PBMA$_{37}$-*b*-PPEGMA$_{39}$ saturated with benzyl acetate. The benzyl acetate concentrations in the aqueous phase were determined at regular time intervals by means of $^1$H NMR spectroscopy. Whereas 70 wt % of the benzyl acetate in the aqueous solution of H40 was released in ~20 h, release of the same weight percentage of benzyl acetate from the H40-PBMA$_{37}$-*b*-PPEGMA$_{39}$ nanocontainer took ~50 h.

## Conclusions

In this contribution, we have described the synthesis of a new class of water-soluble unimolecular containers, which were obtained by sequential ATRP of *n*-butyl methacrylate and poly(ethylene glycol) methyl ether methacrylate, using a 2-bromoisobutyric acid functionalized fourth-generation hyperbranched polyester (Boltorn H40) as the macroinitiator. The average number of arms of the star polymers was determined indirectly via alcoholysis of the polyester core as well as via direct visualization of single star block copolymer molecules with AFM. Using these two techniques, the average number of arms was estimated to be 21 and 16, respectively. DSC and

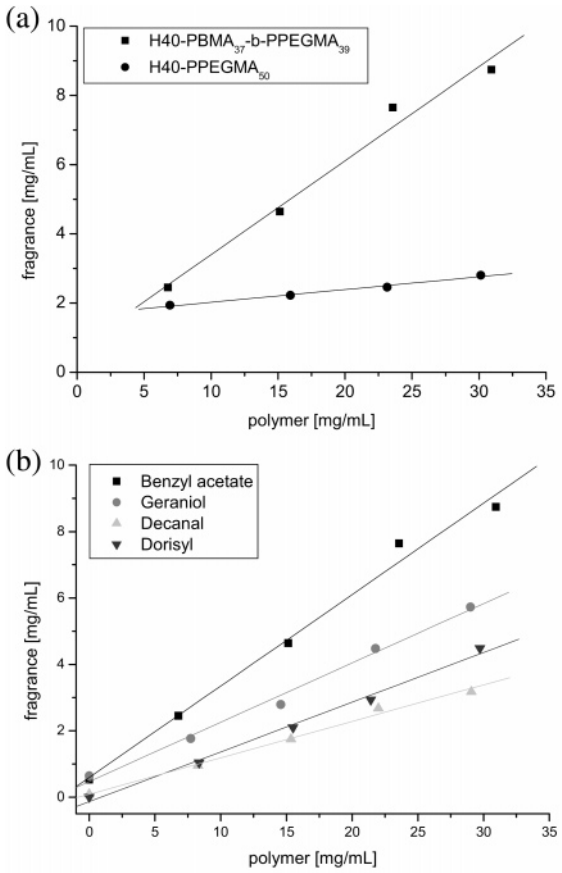


**Figure 11.** (a) Comparison of the benzyl acetate uptake at room temperature of aqueous solutions of H40-PBMA$_{37}$-*b*-PPEGMA$_{39}$ and H40-PPEGMA$_{50}$. (b) Comparison of the uptake of different guest molecules at room temperature into aqueous solutions containing H40-PBMA$_{37}$-*b*-PPEGMA$_{39}$.

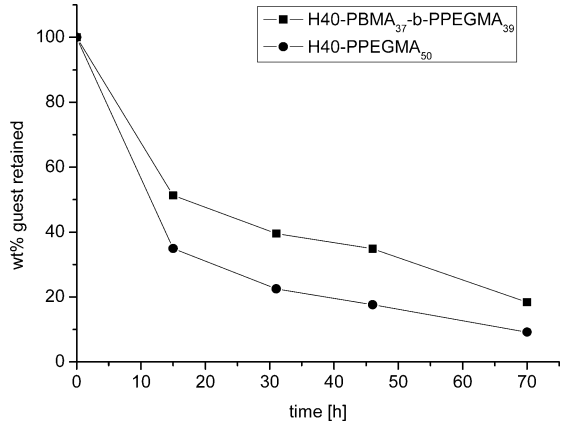


**Figure 12.** Release of benzyl acetate at 50 °C from aqueous solutions of H40-PBMA$_{37}$-*b*-PPEGMA$_{39}$ and H40-PPEGMA$_{50}$.

SAXS experiments on bulk samples indicated a microphase-separated structure, which is in agreement with the core−shell architecture of the star block copolymers. SAXS experiments on aqueous solutions of the star block copolymers indicated that these can be regarded as micelles composed of a corona of Gaussian PPEGMA chains that are attached to a spherical PBMA core. The experimentally determined radii from SAXS were in good agreement with those expected for unimolecular micelles of the H40-PBMA$_x$-*b*-PPEGMA$_y$ star block copolymers. In dilute aqueous solution, these multiarm amphiphilic star block copolymers acted as unimolecular containers that can be loaded with up to 27 wt % hydrophobic guest molecules.

**Acknowledgment.** The CTI Swiss Technology Oriented Program (TOP) Nano 21 and Firmenich SA (Geneva) are acknowledged for financial support. V.C. and I.W.H. are grateful to Pierre Panine for his assistance during SAXS experiments at the ESRF.

## References and Notes

(1) Jones, M.-C.; Leroux, J.-C. *Eur. J. Pharm. Biopharm.* **1999**, *48*, 101.
(2) Kataoka, K.; Harada, A.; Nagasaki, Y. *Adv. Drug Deliv. Rev.* **2001**, *47*, 113.
(3) Patri, A. K.; Majoros, I. J.; Baker, J. R. *Curr. Opin. Chem. Biol.* **2002**, *6*, 466.
(4) Haag, R. *Angew. Chem., Int. Ed.* **2004**, *43*, 278.
(5) Gillies, E. R.; Fréchet, J. M. J. *Drug Discov. Today* **2005**, *10*, 35.
(6) Newkome, G. R.; Moorefield, C. N.; Baker, G. R.; Saunders, M. J.; Grossman, S. H. *Angew. Chem., Int. Ed. Engl.* **1991**, *30*, 1178.
(7) Hawker, C. J.; Wooley, K. L.; Fréchet, J. M. J. *J. Chem. Soc., Perkin. Trans. 1* **1993**, 1287.
(8) Mattei, S.; Seiler, P.; Diederich, F.; Gramlich, V. *Helv. Chim. Acta* **1995**, *78*, 1904.
(9) Stevelmans, S.; van Hest, J. C. M.; Jansen, J. F. G. A.; van Boxtel, D. A. F. J.; de Brabander-van den Berg, E. M. M.; Meijer, E. W. *J. Am. Chem. Soc.* **1996**, *118*, 7398.
(10) Sunder, A.; Krämer, M.; Hanselmann, R.; Mülhaupt, R.; Frey, H. *Angew. Chem., Int. Ed.* **1999**, *38*, 3552.
(11) Krämer, M.; Stumbé, J.-F.; Türk, H.; Krause, S.; Komp, A.; Delineau, L.; Prokhorova, S.; Kautz, H.; Haag, R. *Angew. Chem., Int. Ed.* **2002**, *41*, 4252.
(12) Morgan, M. T.; Carnahan, M. A.; Immoos, C. E.; Ribeiro, A. A.; Finkelstein, S.; Lee, S. J.; Grinstaff, M. W. *J. Am. Chem. Soc.* **2003**, *125*, 15485.
(13) Fuchs, S.; Kapp, T.; Otto, H.; Schöneberg, T.; Franke, P.; Gust, R.; Schlüter, A. D. *Chem.—Eur. J.* **2004**, *10*, 1167.
(14) Narrainen, A. P.; Pascual, S.; Haddleton, D. M. *J. Polym. Sci., Part A: Polym. Chem.* **2002**, *40*, 439.
(15) Cloutet, E.; Fillaut, J.-L.; Astruc, D.; Gnanou, Y. *Macromolecules* **1999**, *32*, 1043.
(16) Hedrick, J. L.; Trollsås, M.; Hawker, C. J.; Atthoff, B.; Claesson, H.; Heise, A.; Miller, R. D.; Mecerreyes, D.; Jerome, R.; Dubois, Ph. *Macromolecules* **1998**, *31*, 8691.
(17) Jia, Z.; Zhou, Y.; Yan, D. *J. Polym. Sci., Part A: Polym. Chem.* **2005**, *43*, 6534.
(18) Xu, J.; Luo, S.; Shi, W.; Liu, S. *Langmuir* **2006**, *22*, 989.
(19) Zhou, G.; Smid, J. *Langmuir* **1993**, *9*, 2907.
(20) Chen, X.; Smid, J. *Langmuir* **1996**, *12*, 2207.
(21) Park, S. Y.; Han, B. R.; Na, K. M.; Han, D. K.; Kim, S. C. *Macromolecules* **2003**, *36*, 4115.
(22) Teng, J.; Zubarev, E. R. *J. Am. Chem. Soc.* **2003**, *125*, 11840.
(23) Xu, J.; Zubarev, E. R. *Angew. Chem., Int. Ed.* **2004**, *43*, 5491.
(24) Huh, J.; Kim, K. H.; Ahn, C.-H.; Jo, W. H. *J. Chem. Phys.* **2004**, *121*, 4998.
(25) Jones, M.-C.; Ranger, M.; Leroux, J.-C. *Bioconjugate Chem.* **2003**, *14*, 774.
(26) Wang, F.; Bronich, T. K.; Kabanov, A. V.; Rauh, R. D.; Roovers, J. *Bioconjugate Chem.* **2005**, *16*, 397.
(27) Haddleton, D. M.; Kukulj, D.; Duncalf, D. J.; Heming, A. M.; Shooter, A. J. *Macromolecules* **1998**, *31*, 5201.
(28) Pedersen, J. S. *J. Appl. Crystallogr.* **1994**, *27*, 595.
(29) *Small-Angle X-ray Scattering*; Glatter, O., Kratky, O., Eds.; Academic Press: London, 1982.
(30) Prosa, T. J.; Bauer, B. J.; Amis, E. J. *Macromolecules* **2001**, *34*, 4897.
(31) Willner, L.; Jucknischke, O.; Richter, D.; Roovers, J.; Zhou, L. L.; Toporowski, P. M.; Fetters, L. J.; Huang, J. S.; Lin, M. Y.; Hadjichristidis, N. *Macromolecules* **1994**, *27*, 3821.
(32) Pedersen, J. S. *J. Chem. Phys.* **2001**, *114*, 2839.
(33) Pedersen, J. S.; Gerstenberg, M. C. *Macromolecules* **1996**, *29*, 1363.
(34) Perstorp product data sheet, Boltorn H40, http://www.perstorp.com.
(35) Angot, S.; Murthy, K. S.; Taton, D.; Gnanou, Y. *Macromolecules* **1998**, *31*, 7218.
(36) Ohno, K.; Wong, B.; Haddleton, D. M. *J. Polym. Sci., Part A: Polym. Chem.* **2001**, *39*, 2206.
(37) Haddleton, D. M.; Duncalf, D. J.; Kukulj, D.; Heming, A. M.; Shooter, A. J.; Clark, A. J. *J. Mater. Chem.* **1998**, *8*, 1525.
(38) Haddleton, D. M.; Crossman, M. C.; Dana, B. H.; Duncalf, D. J.; Heming, A. M.; Kukulj, D.; Shooter, A. J. *Macromolecules* **1999**, *32*, 2110.
(39) Yan, F.; Déjardin, P.; Frère, Y.; Gramain, P. *Makromol. Chem.* **1990**, *191*, 1197.
(40) Bo, G.; Wesslén, B.; Wesslén, K. B. *J. Polym. Sci., Part A: Polym. Chem.* **1992**, *30*, 1799.
(41) *Polymer Handbook*, 3rd ed.; Brandup, J., Immergut, E. H., Eds.; John Wiley & Sons: New York, 1989; p VI/217.
(42) Castelletto, V.; Caillet, C.; Fundin, J.; Hamley, I. W.; Yang, Z.; Kelarakis, A. *J. Chem. Phys.* **2002**, *116*, 10947.
(43) Acros Organics, Material Safety Data Sheet Benzyl acetate, www.acros.be.

MA060548B